Thermoacoustic analysis of lean H$_2$-air premixed flames in thin layers

F. Veiga-López[1], D. Martínez-Ruiz[2], M. Kuznetsov[3] and M. Sánchez-Sanz[1]

[1]Depto. de Ing. Térmica y de Fluidos, Univ. Carlos III de Madrid, 28911, Leganés, España

[2]Depto. de Mec. de Fluidos y Prop. Aeroespacial, UPM, 28040, Madrid, España

[3]Karlsruhe Institut für Technologie, 76344, Eggenstein-Leopoldshafen, Deutschland

1   Introduction

Thermoacoustic instability appears as a result of the coupling between a reactive front and the pressure waves present in a combustion chamber. Previous experimental studies mostly investigated the behavior of premixed downward-propagating flames in axysimmetric geometries [1–4]. Two main regimes were found by all these authors: the primary and secondary (parametric) acoustic oscillatory flames, as a result of the aforementioned feedback mechanism. Recently, Veiga-López et al. [5] analyzed thermoacoustics in an horizontal Hele-Shaw cell for a set of hydrocarbons. Aldredge et al. [4] and Veiga-López et al. [5] introduce the importance of the Markstein number on the different acoustic-flame interaction regimes. Here, we further analyze thermoacoustic instabilities in a quasi-2D geometry for lean hydrogen-air premixed flames propagating downwards towards a closed end. The importance of the equivalence ratio as well as the role played by the channel thickness is reported in this paper.

2   Experimental Setup and Procedure

The experimental setup sketched in Figure 1 was built for this purpose. A vertical combustion chamber is conformed by two 10-mm-thick flat plexiglass plates separated by a PVC sealing hollow frame. The total volume enclosed by the cell is 900 x 200 x (10-4) mm^3 ($L \times W \times h$). The gap height (h) can be modified to assess its effect.
Fuel and oxidant are mixed before entering the combustion chamber, controlling the fuel-to-air ratio with two EL-FLOW mass flow controllers. The mixture is fed via an injection port located at the top ignition side of the chamber, keeping this end closed and opening the venting valve. The complete charge of the chamber is checked at the outlet line using a gas analyzer Rosemount^{TM} CT5400. After a minute of exposure, the top end is fully reopened and the mixture ignited simultaneously by a spark plug. A Z-shape Schlieren system is used to capture high-speed images of the flame front. A LED light source, two 280-mm-diameter mirrors,
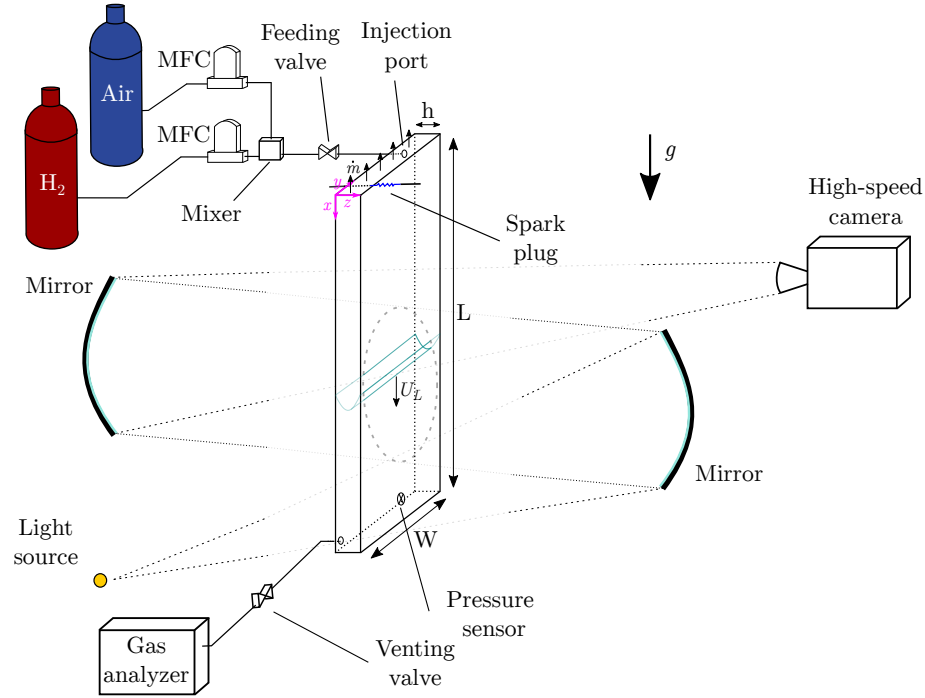
Figure 1: Schematic of the experimental setup. Z-shape Schlieren system used for image acquisition. The dimensions of the cell are $L \times W \times h$. The black arrows at the top end of the chamber represent the unobstructed release of the combustion products.

a set of lenses and a high-speed camera (Photron FASTCAM SA 1.1) form the optical system. Due to the limited size of the mirrors, only partial visualization of the flame was possible during each experiment. The chamber can be shifted vertically to change the region of interest, thus capturing the whole channel length in several trials. Additionally, a pressure sensor (PCB M113B12) is located at the bottom of the chamber to measure the inner over-pressure. Finally, the reader can consult the main properties of the analyzed flames in [2].

3   Results

The effect of the equivalence ratio ϕ is assessed by keeping a constant 10-mm gap. For mixtures with an equivalence ratio lower than a critical value, $\phi \leq \phi_c = 0.36$, the flame experiences violent oscillations as a result of the coupling with acoustic waves present in the chamber. These oscillations can be compared to those found by Veiga-Lopez et al. [5] for rich (lean) propane and DME (methane) mixtures propagating in a similar geometry. The left part of Figure 2(a) shows the characteristic velocity footprint left by a $\phi = 0.26$ hydrogen-air flame. Note that because of a limited visualization region, a discontinuous signal was obtained. Furthermore, the left part of Figure 2(b) represents the over-pressure within the combustion chamber, upholding the coupling between flame and acoustics. In this case, the over-pressure rises up to 3 kPa giving associated maximum flame velocities of around 4 m/s.
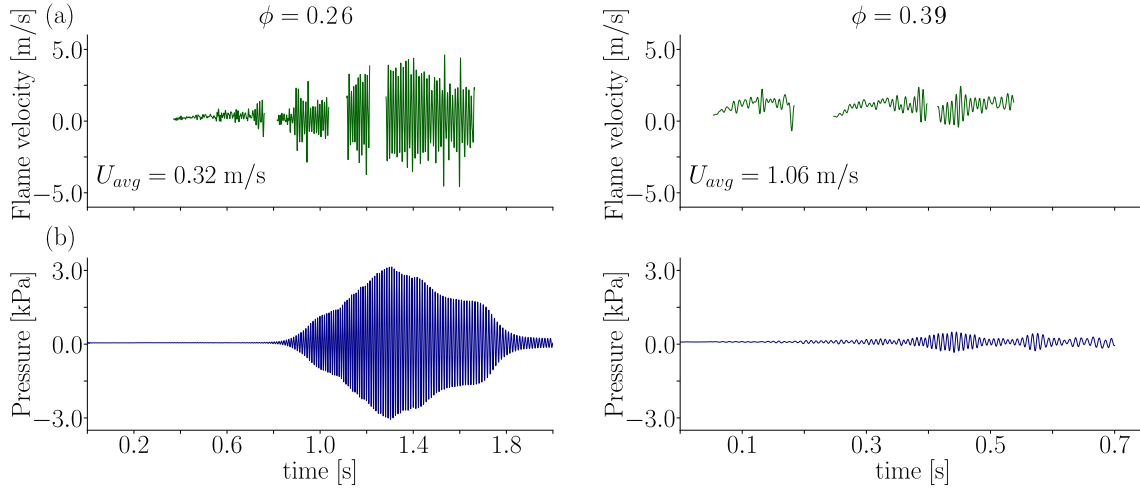
Figure 2: (a) Characteristic flame velocity with time calculated from the burned volume ($U_L = (Hh)^{-1}dV_b/dt$) for leaner (left) and richer (right) hydrogen flames than $\phi_c = 0.36$. (b) Over-pressure signal at the interior of the chamber.
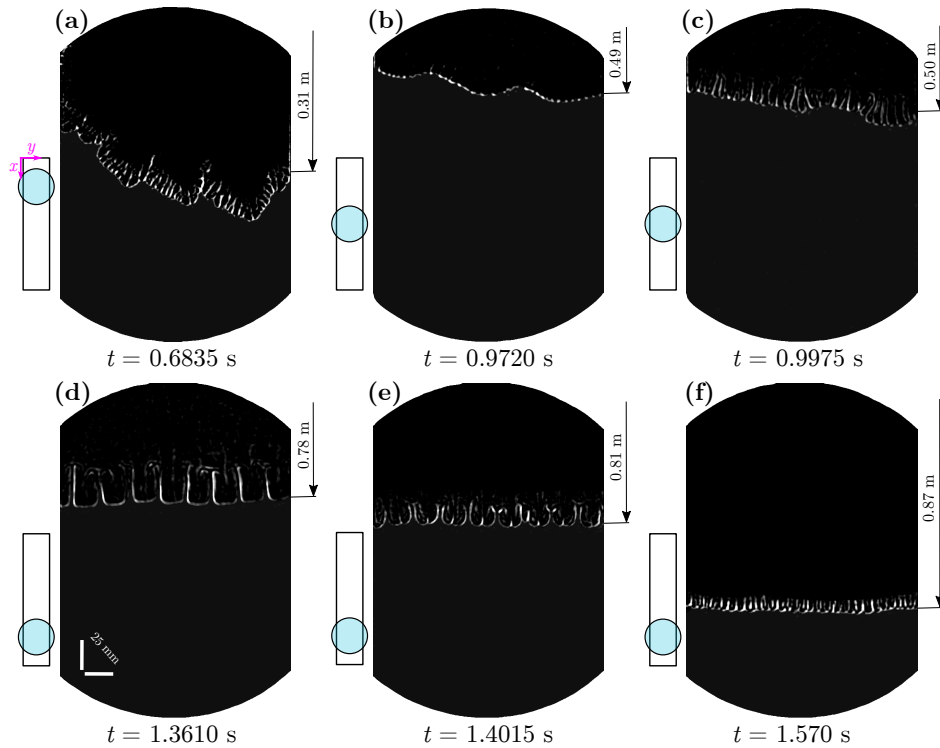
Figure 3: Shadow images of a flame propagating in the secondary acoustic oscillations regime ($\phi = 0.26 < \phi_c$) captured at different times, t. The scheme at the left of each image represents the region captured during the experiment. The arrow at the right indicates the approximate vertical position of the mid-point of the front measured from the open top end.

Figure 3(a)-(f) are several snapshots of a secondary (parametric) acoustic instability experiment. Once ignited, the flame soon rumples due to hydrodynamic and thermodiffusive instabilities reminding of very wrinkled petals (a). Further down (b), determined frequencies ($f \approx 85 - 105\ Hz$) of the ignition noise are amplified by the presence of the reactive front, undergoing a feedback mechanism. Here, the flame becomes almost planar and oscillates at the acoustic frequency with a low-amplitude ($|U_L| < 0.75\ m/s$) motion. Shortly (c), the pressure waves are further magnified triggering the transition to the secondary regime, making it possible to observe small wrinkles ($\lambda_{\phi=0.26} \approx 6.5\ mm$) forming on top of the planar front. Under the effect of such high-amplitude pressure waves (d-e), the outline of the flame changes drastically. It forms characteristic regular wrinkles bigger than before ($\lambda_{\phi=0.26} \approx 25\ mm$), with long funnels penetrating towards the hot products. The flame oscillates at the acoustic frequency with velocity peaks of ($|U_L| \approx 4\ m/s$). At the next period, the tips at the mid position of the flame cells now form the long funnels, resulting in a period doubling at these particular points (mid-points of the cells and funnels). Nevertheless, the average frequency of the motion matches that of the pressure waves. Finally (f), the amplitude of the movement is reduced as well as the size of the wrinkles, recovering that of the transition.

(a)	(b)	(c)
$t = 0.0810\ s$	$t = 0.3575\ s$	$t = 0.5850\ s$
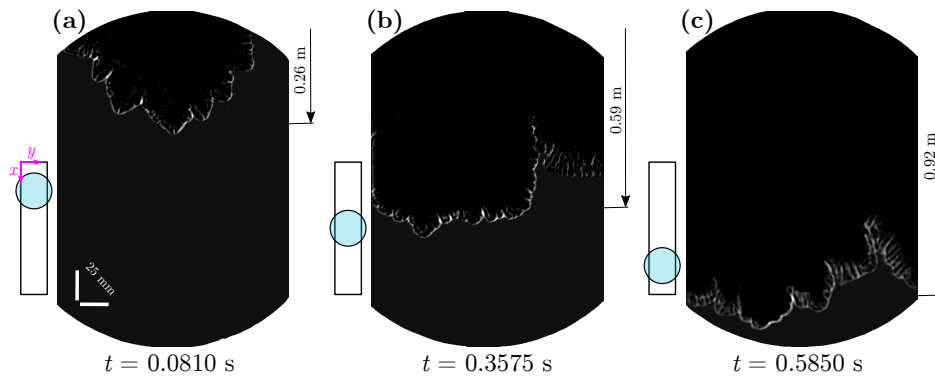
Figure 4: Shadow images of a flame propagating in the primary acoustic oscillations regime ($\phi = 0.39 > \phi_c$) captured at different times, t.

For H$_2$-air mixtures richer than ($\phi_c = 0.36$) only primary acoustic oscillations are observed. The right part of Figure 2 shows the characteristic velocity observed in a flame with $\phi = 0.39$ (a) and the over-pressure within the chamber (b). Figure 4(a)-(c) were taken from videos of flames propagating under the primary acoustic instability. At the beginning (a), the flame shows a similar petal-like shape to that of the preceding example. At approximately the half of the combustion chamber (b), the front experiences small-amplitude ($|U_L| \approx 0.5\ m/s$) oscillations with a frequency of $f \approx 135\ Hz$ that make the front planar, lasting until the end of the chamber (c).

Additionally, the effect of the gap size (h) on the flames propagation was analyzed by changing the frame thickness from 10 to 4 mm with a 2-mm step. Figure 5(a) and (b) show, respectively, the variation of the maximum chamber pressure and the peak frequency of the pressure signals with equivalence ratio for different gap sizes. The frequency of the acoustic waves is slightly reduced as well as the over-pressure within the channel when reducing h. The reason behind it seems to point towards viscous dissipation in the vicinity of the walls and heat losses to the solid surface. The smaller the gap, the higher energy dissipation due to the increased relative size of the acoustic boundary layer and heat losses. Moreover, the transition to the secondary acoustic oscillations happens for leaner mixtures, which could also be due to energy dissipation. The critical equivalence ratio shifts from $\phi_c \approx 0.36$ ($h = 10$ mm) to $\phi_c \approx 0.32$ ($h = 4$ mm). We consider that a flame experiences secondary acoustic oscillations when the over pressure peak exceeds 1 kPa and the

flame position shows a sudden slope change [5].
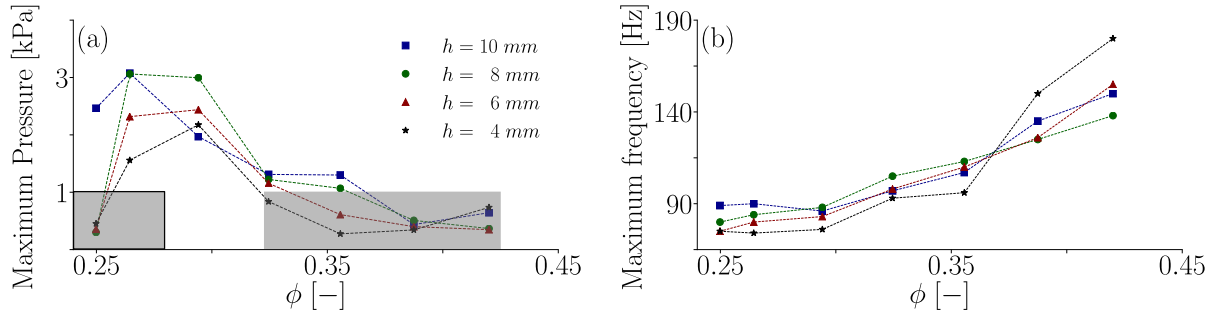
Figure 5: (a) Variation with ϕ of the maximum acoustic over-pressure at the channel for different gap sizes (h). The shadowed areas of the graph represent the primary acoustic instability regime regions. (b) Effect of ϕ to the maximum oscillation frequency for different (h).

Furthermore, for channels with $h \leq 8$ mm the pressure waves are highly attenuated due to energy losses when $\phi \leq 0.25$, recovering the primary acoustic oscillations. Figure 6 shows two characteristic images of such a flame propagating at a 4-mm gap size. It behaves as explained before for thicker channels. One important feature is the appearance of quenched areas in the domain, a symptom of the importance of heat losses when close to the flammability limit.
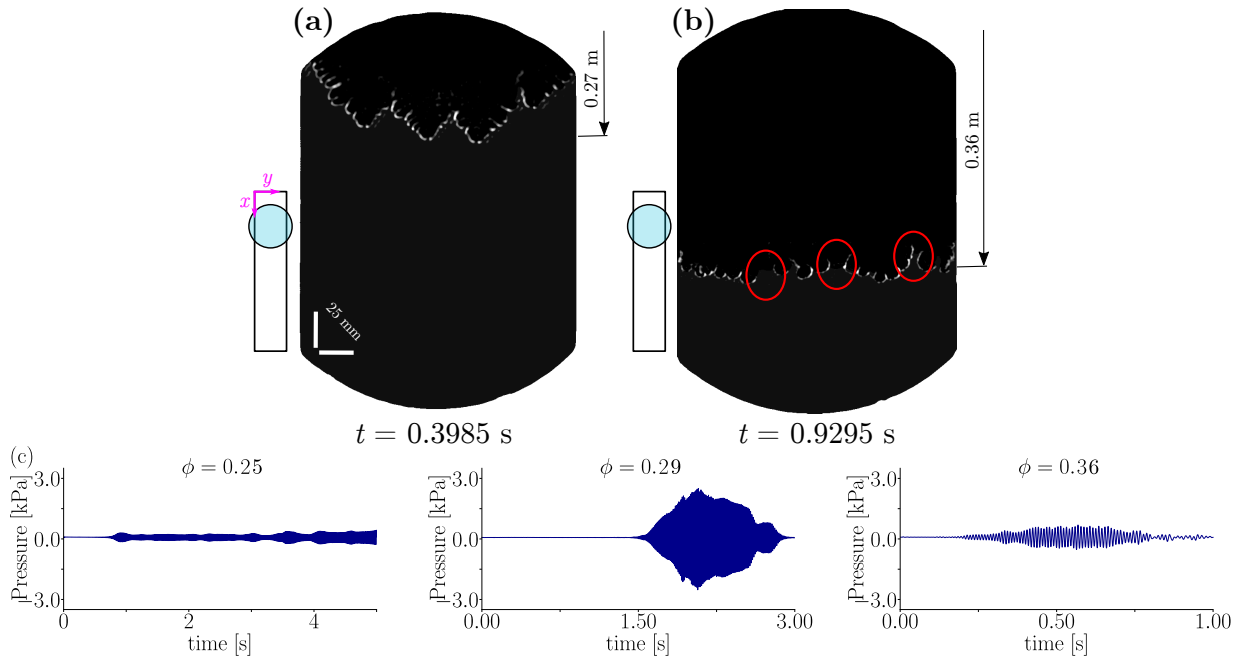
Figure 6: (a)-(b) Post-processed shadow images of a flame propagating in the new primary acoustic oscillations regime for $\phi = 0.25$ and $h = 4$ mm. The red circles remark the partially-quenched areas. (c) Over-pressure signals obtained in the interior of a $h = 6$ mm chamber for different ϕ.

4   Conclusions

Thermoacoustic instabilities in narrow channels is studied experimentally for very lean hydrogen-air pre-mixed flames. In particular, the effect of the equivalence ratio ϕ and the channel thickness h on the transition from the primary to the secondary regime is assessed. During the primary acoustic oscillations, the flame remains mostly unperturbed by the pressure waves. It flattens and oscillates at a certain frequency until it reaches the end of the channel. When the regime changes, the front experiences violent oscillations and presents a characteristic finger-like shape.

Regarding the effect of the equivalence ratio, the transition from primary to secondary acoustic oscillations happens for mixtures leaner than $\phi_c = 0.36$. This point corresponds to a critical Markstein number of $\mathcal{M}_c = -1.17$ under the prescribed geometrical conditions (i.e. $h = 10$ mm). The Markstein number is the best candidate to control the transition between the two described regimes because of its monotonic variation with equivalence ratio, decreasing for leaner mixtures. This points out the importance of flame stretch on triggering the secondary thermoacoustic instability.

Furthermore, the effect of the combustion chamber thickness was studied by varying h from 10 mm down to 4 mm. The maximum acoustic pressure reduces for thinner channel as the viscous losses become more important. Likewise, the transition from the primary to secondary regimes appears at leaner hydrogen-air mixtures. Additionally, the primary acoustic oscillations are recovered for channels whose thickness is $h \leq$ 8 mm for very lean ($\phi = 0.25$) mixtures.

5   Acknowledgments

References

[1] G. Searby, "Acoustic instability in premixed flames," *Combustion Science and Technology*, vol. 81, no. 4-6, pp. 221–231, 1992.

[2] J. Yanez, M. Kuznetsov, and J. Grune, "Flame instability of lean hydrogen–air mixtures in a smooth open-ended vertical channel," *Combustion and Flame*, vol. 162, no. 7, pp. 2830–2839, 2015.

[3] S. H. Yoon, T. J. Noh, and O. Fujita, "Onset mechanism of primary acoustic instability in downward-propagating flames," *Combustion and Flame*, vol. 170, pp. 1–11, 2016.

[4] R. C. Aldredge and N. Killingsworth, "Experimental evaluation of markstein-number influence on ther-moacoustic instability," *Combustion and flame*, vol. 137, no. 1-2, pp. 178–197, 2004.

[5] F. Veiga-López, D. Martínez-Ruiz, E. Fernández-Tarrazo, and M. Sánchez-Sanz, "Experimental analy-sis of oscillatory premixed flames in a hele-shaw cell propagating towards a closed end," *Combustion and Flame*, vol. 201, pp. 1–11, 2019.